Body mass index in relation to extracellular vesicle–linked microRNAs in human follicular fluid

Rosie M. Martinez, Sc.D., M.P.H.,[a,c] Andrea A. Baccarelli, M.D., Ph.D.,[c] Liming Liang, Ph.D.,[b] Laura Dioni, Ph.D.,[d] Abdallah Mansur, M.S.,[e] Michal Adir, Bs.C.,[e] Valentina Bollati, M.D.,[d] Catherine Racowsky, Ph.D.,[f] Russ Hauser, M.D., Sc.D.,[a] and Ronit Machtinger, M.D.[e]

[a] Department of Environmental Health and [b] Department of Biostatistics, Harvard T.H. Chan School of Public Health, Boston, Massachusetts; [c] Laboratory of Precision Environmental Biosciences, Department of Environmental Health Sciences, Columbia Mailman School of Public Health, New York, New York; [d] Epidemiology, Epigenetics, and Toxicology Laboratory, Department of Clinical Sciences and Community Health, University of Milan, Milan, Italy; [e] Department of Obstetrics and Gynecology, Sheba Medical Center and Sackler School of Medicine, Tel-Aviv University, Ramat-Gan, Israel; and [f] Department of Obstetrics, Gynecology, and Reproductive Biology, Brigham and Women's Hospital, Harvard Medical School, Boston, Massachusetts.

Objective: To study whether increased body mass index is associated with altered expression of extracellular vesicle microRNAs (EV-linked miRNAs) in human follicular fluid.
Design: Cross-sectional study.
Setting: Tertiary-care university-affiliated center.
Patient(s): One hundred thirty-three women undergoing in vitro fertilization (IVF) were recruited from January 2014 to August 2016.
Interventions(s): None.
Main Outcome Measure(s): EV-linked miRNAs were isolated from follicular fluid and their expression profiles were measured with the use of the Taqman Open Array Human miRNA panel. EV-linked miRNAs were globally normalized and inverse-normal transformed. Associations between body mass index (BMI) and EV-linked miRNA outcomes were analyzed by means of multivariate linear regression and principal component analysis.
Result(s): Eighteen EV-linked miRNAs were associated with an increase in BMI after adjusting for age, ethnicity, smoking status, and batch effects. Hsa-miR-328 remained significant after false discovery rate adjustments. Principal component analyses identified the first principal component to account for 40% of the variation in our EV-linked miRNA dataset, and adjusted linear regression found that the first principal component was significantly associated with BMI after multiple testing adjustments. Using Kyoto Encyclopedia of Genes and Genomes enrichment analyses, we predicted gene targets of EV-linked miRNA in silico and identified PI3K-Akt signaling, ECM-receptor interaction, focal adhesion, FoxO signaling, and oocyte meiosis pathways.
Conclusion(s): These results show that a 1-unit increase in BMI is associated with altered follicular fluid expression of EV-linked miRNAs that may influence follicular and oocyte developmental pathways. Our findings provide potential insight into a mechanistic explanation for the reduced fertility rates associated with increased BMI. (Fertil Steril® 2019;112:387–96. ©2019 by American Society for Reproductive Medicine.)
El resumen está disponible en Español al final del artículo.

Key Words: IVF, microRNAs, extracellular vesicles, BMI

Human infertility is influenced by a broad range of physical, hormonal, genetic, and environmental stressors (1). Despite enormous advances in the technical aspects of in vitro fertilization (IVF), the success rates of the procedure remain relatively low. Whereas much has been published about nonmodifiable factors associated with outcomes of IVF, such as female age, fertility diagnosis, and ovarian reserve, less attention has been devoted to modifiable

Received September 7, 2018; revised March 28, 2019; accepted April 1, 2019; published online May 27, 2019.
R.M.M. has nothing to disclose. A.A.B. has nothing to disclose. L.L. has nothing to disclose. L.D. has nothing to disclose. A.M. has nothing to disclose. M.A. has nothing to disclose. V.B. has nothing to disclose. C.R. has nothing to disclose. R.H. has nothing to disclose. R.M. has nothing to disclose.
Supported by the National Institutes of Environmental Health Sciences (grant R21-ES024236); Israel Science Foundation (grant 1936/12); the Environment and Health Fund, Israel (grant 1301); and Education and Research Center for Occupational Safety and Health CDC/NIOSH (grant award T42/OH008416).
Reprint requests: Ronit Machtinger, M.D., Department of Obstetrics and Gynecology, Sheba Medical Center, Tel-Aviv University, Ramat-Gan, Israel 52561 (E-mail: ronit.machtinger@sheba.health.gov.il).

Fertility and Sterility® Vol. 112, No. 2, August 2019 0015-0282/$36.00

https://doi.org/10.1016/j.fertnstert.2019.04.001

behavioral risk factors, such as body mass index (BMI), that may influence IVF outcomes (2–4).

Studies have shown that an increased BMI and obesity alter follicular development, oocyte maturation, and reduced numbers of oocytes retrieved (5–9). Women with BMIs ≥ 25 kg/m^2 undergoing IVF have a significantly reduced chance of a clinical pregnancy compared with women with BMIs <25 kg/m^2 (10–12). Despite the ample epidemiologic evidence, the molecular mechanisms underlying how increased BMI contributes to infertility are still unknown.

The ovarian follicle houses the oocyte itself, and as it matures cellular differentiation occurs, creating cellular layers of thecal, mural granulosa, and cumulus cells. Theca and granulosa cells create the membrane of the follicle itself, and cumulus cells encapsulate the oocyte (13, 14). Follicular fluid (FF) is a crucial microenvironment for the developing oocytes, containing hormones, metabolites, ions, proteins, and various biologic structures, including noncoding RNAs and extracellular vesicles (EVs) (14–21). EVs, membrane-enclosed structures (22), have been identified as a means for intercellular communication between the granulosa cells and oocyte in the FF (15). They are nanosized (30–700 nm in diameter) and can contain numerous molecules involved in cell signaling and cell-to-cell communication, including microRNAs (miRNAs), which are short noncoding RNA molecules (~22 nucleotides long) (23). MiRNAs can post-transcriptionally regulate gene expression (24–26) and can be free-floating or packaged in EVs (EV-linked miRNAs). Extracellular vesicles (exosomes, microvesicles, and other membrane-bound vesicles) have been detected in almost every biofluid, including FF (22), and can act as a vehicle carrying proteins, messenger RNAs (mRNAs), and miRNAs (27). These EV-linked miRNAs can be encapsulated within the EV itself as well as also associated with the EV extracellularly (28). These EV-linked miRNAs can influence gene expression and may be important for follicular signaling (15, 29, 30).

Several studies have reported possible associations between BMI and EV-linked miRNA profiles in either adipocytes or serum, linking some of these EV-linked miRNAs with pathways of inflammation and insulin resistance (31–34). To the best of our knowledge, no study has examined associations between BMI and EV-linked miRNAs found in FF. Investigating EV-linked miRNAs in FF might help to elucidate the mechanisms and pathways by which these modified risk factors that can impact fertility. Therefore, the present study aimed to investigate the effects of BMI with EV-linked miRNA expression isolated from FF in women undergoing IVF treatment.

MATERIALS AND METHODS

Ethics

This study was approved by the Sheba Medical Center Institutional Review Board in accordance with the Declaration of Helsinki (35). All participants provided written informed consent at enrollment.

Study Population

From January 2014 to August 2016, women undergoing IVF were recruited in a tertiary-care university-affiliated hospital. Eligibility criteria were women aged 19–38 years, undergoing their first to sixth IVF attempt with basal FSH <10 IU. To avoid potential confounding by the stimulation regimen or fertility diagnosis, we enrolled only women who were treated with the use of GnRH antagonist protocol as well as women undergoing IVF due to unexplained infertility, with mild male factors, and undergoing IVF for pregestational diagnosis of autosomal recessive disorders. We excluded those with a diagnosis of polycystic ovarian syndrome, endometriosis, or poor response according to the Bologna criteria (36) which might impair oocyte quality. All women contributed a single IVF cycle.

Exposure Assessment

Each participant's height and weight were measured at the beginning of the IVF cycle and were used to calculate BMI by dividing the weight with the square of the height (kg/m^2).

Outcome Assessment

RNA extraction from follicular fluid. Follicular fluid (otherwise discarded material) was collected during oocyte retrieval from a single follicle >18 mm per patient and centrifuged at 1,500*g* for 15 minutes. FF was aliquoted to 0.5-mL tubes so that the volumes of FF that were analyzed were equivalent among patients. Samples were precleaned with the use of a 0.80-μm-pore polyethersulfone filter (StericupRVP; Merck Millipore) to remove larger proteins and debris and aliquoted into 500 μL for immediate storage at -80°C (37). Only mature (metaphase II) oocytes were examined for RNA analysis. Methods for RNA extraction from biologic fluids have been previously described (38). In short, samples were thawed, centrifuged for 15 minutes at 1,200*g* at room temperature, and then centrifuged at 1,000*g*, 2,000*g*, and 3,000*g* for 15 minutes each at 4°C. Following this step, samples were ultracentrifuged (Beckman Coulter Optima-MAX-XP) at 110,000*g* for 75 minutes at 4°C for the extraction of EV, because ultracentrifugation is considered to be the standard according to International Society for Extracellular Vesicle recommendations (28, 39). The pellets obtained were kept at -80°C until use. EV-linked miRNAs were extracted from the ultracentrifuged pellets with the use of the miRNAeasy Kit and RNeasy Cleanup Kit per the manufacturer (Qiagen). The final purified EV-linked miRNA-enriched RNA was eluted into 20 μL RNAse-free water and stored at -80°C until further use. This protocol had been tested and samples were examined with the use of both Nanosight and flow cytometry for CD63 (an EV-specific marker; results unpublished).

Expression analysis of EV-Linked miRNAs in follicular fluid. We screened for 754 miRNAs with the use of the Taqman Open Array system. We obtained 758 relative cycle threshold (Crt) values for each FF sample, which included 754 unique miRNAs and four internal control samples (ath-miR159a, RNU48, RNU44, and U6). Methods of real-time quantitative polymerase chain reaction (RT-qPCR) for

screening EV-linked miRNAs with the use of the miRNA array in biologic fluids are published elsewhere (38). Quantstudio 12K Flex is a fixed-content panel containing validated human Taqman MicroRNA Assays derived from Sanger miRBase release v.14. All 754 assays have been functionally validated with the use of miRNA artificial templates. The panel is specifically designed to provide specificity for only the mature miRNA targets. Taqman MicroRNA Assays (spotted in the panel) incorporate a target-specific stem–loop reverse-transcription primer allowing the assay to work despite the short length of mature miRNAs (~22 nucleotides) which prohibits conventional design of primers. Briefly, we prepared 3.3 μL of each RNA sample and then reverse-transcribed to complementary DNA and preamplified. Preamplified samples were mixed with the Taqman Open Array Real-Time PCR Master Mix (Life Technologies) and loaded onto a Taqman Open Array Human miRNA panel with the use of the Quantstudio Accufill System Robot (Life Technologies). RT-qPCR was performed on the Quantstudio 12K Flex Real-Time PCR System with the use of the Open Array Platform (QS12KFLEX; Life Technologies) according to the manufacturer's instructions. Expression levels were calculated in Crt values, estimating the amplification cycle at which the fluorescence levels for each of the analyzed EV-linked miRNAs exceed the background fluorescence threshold (40).

Covariate Assessment

Each participant's age, number of previous IVF attempts, and number of oocytes retrieved at the start of IVF cycle were extracted from her medical charts. Cigarette smoking status was determined by a questionnaire in which participants were asked about cigarette smoking history and intensity. Smoking status was categorized as never smoker, former smoker, or current smoker. Those who self-identified as former smokers had stopped smoking before the beginning of their IVF cycle. FF samples were analyzed for EV-linked miRNAs in two batches, and in our subsequent statistical analyses we controlled for batch (batch 1 vs. batch 2).

Statistical Analysis

Descriptive statistics and normalization of EV-Linked miRNAs. Thermo Fisher Cloud Relative Quantification software was used to extract the EV-linked miRNA qPCR data. To ensure accuracy of in our normalization methods of the EV-linked miRNAs, we ran algorithms to identify the best normalization strategy. We first applied the NormFinder and geNorm algorithms to select the best normalization strategy among global mean (arithmetic and geometric), RNU48, RNU6, or the average of the four miRNAs with the lowest standard deviation (SD) among subjects. Based on these algorithms, we found that global mean was the best method to normalize the data. EV-linked miRNAs data was normalized using the global mean (GM) method: ΔCrt EV-linked miRNAi = Crt EV-linked miRNAi − Crt EV-linked miRNAi global mean (38). All of the EV-linked miRNA with a Crt value >28 or amplification score ≤1.24 were identified as unexpressed. For the global mean, we coded all those EV-linked miRNAs that were unexpressed as 28, as suggested by Pergoli et al. (38). We calculated ΔCrt based on the global mean across all of the miRNAs within that subject and dividing it by the total miRNAs (n = 754). All subsequent analyses were performed exclusively on those EV-linked miRNAs that had expressed values detected in ≥15% of our samples, based on the histogram distribution of the percentage detected in our samples (Supplemental Fig. 1 and Supplemental Table 1 available online at www.fertstert.org). This cutoff was chosen to maximize the number of EV-linked miRNAs examined while retaining a large enough sample to assess the associations (≥20 individuals) and removing those EV-linked miRNAs that had a very large missing rate. Standard descriptive statistics were used to explore the characteristics of the study participants and exposure data. Spearman correlation coefficients were used to examine correlations between covariates and exposure variables.

EV-linked miRNA by EV-linked miRNA regression analysis. Linear regression models were performed to elucidate top-hit EV-linked miRNAs. Models were adjusted for continuous age (years), continuous BMI, categoric smoking status, binary race/nationality, binary batch, and continuous surrogate variables identified by the surrogate variable analysis (SVA) package in R. The SVA package can help to identify and remove any batch effects or unwanted sources of variation, seasonal, meteorologic, exposure, or technical variables, which are unknown but might be differently distributed in the two batches of samples (41, 42). EV-linked miRNA outcomes were inverse normally transformed to ensure normality with a standard deviation of 1. To account for multiple testing, we applied the Benjamini-Hochberg false-discovery rate (FDR) p.adjust function in R (43). All statistical analyses were performed in R version 3.4.0 (44). Statistical significance was set at $P<.05$.

Principal Component Analysis

Principal component analyses (PCA) were performed to examine the overall variation of EV-linked miRNA profiles. All of the selected 192 EV-linked miRNAs were included in the analysis. The prcomp function in R was used to calculate the principal components (PCs) and the PC loadings for each component. All variables were scaled and centered with a mean of 0 and a standard deviation of 1 before the PCA. PCs were inverse normally transformed for normality. Separate unadjusted univariate analyses were performed on age, smoking status, and BMI by means of linear regression with each principal component as the outcome. Mutually adjusted linear regressions were performed with the principal components as the outcomes and adjusted for age, BMI, smoking status, race, batch, and SVA surrogate variables. Absolute values of the PC loadings were taken and the EV-linked miRNAs that contributed a loading in the 90th percentile or higher were examined further. This threshold was chosen based on both the histogram distribution of the absolute values of the PC loadings (Supplemental Fig. 2) and the percentile cutoffs (Supplemental Table 2). This would allow us to examine those EV-linked miRNAs that are the most important to the

TABLE 1

Patients' demographic characters (n = 133).

Variable	Data
Age, y	30.9 ± 3.7
BMI, kg/m^2	23.6 ± 4.7
Number of oocytes retrieved	9.4 ± 5.1
WHO BMI categories	
Underweight	15 (11)
Normal	73 (56)
Overweight	31 (23)
Obese	14 (10)
Smoking status	
Never smoker	72 (54)
Ever smoker	27 (20)
Current smoker	34 (26)
IVF attempts	
First attempt	87 (65)
Attempt >1	46 (35)
Ethnicity	
Caucasian	122 (92)
Asian	8 (6)
African	1 (1)
Hispanic	2 (1)
Diagnosis	
PGD	57 (43)
Male factor	53 (40)
Unexplained	20 (15)
Other	3 (2)
Pre-IVF fertility status	
Fertile	58 (44)
Infertile	75 (56)

Note: Values represent mean ± standard deviation or n (%). BMI = body mass index; IVF = in vitro fertilization; PGD = pregestational diagnosis; WHO = World Health Organization.

Martinez. BMI and EV-linked microRNAs. Fertil Steril 2019.

principal component while keeping the number of EV-linked miRNAs manageable.

Kyoto encyclopedia of genes and genomes pathway analysis. An in silico analysis with the use of a web-based tool, miRWalk2.0 (mirwalk.umm.uni-heidelberg.de) was performed to investigate gene targets of EV-linked miRNAs (45). Target predictions included a comparative analysis of seven prediction programs: DIANAmT, miRanda, miRDB, miRWalk, PICTAR5, RNA22, and Targetscan. To decrease the number of false positive pathways, targeted genes were identified that were validated in a total of five prediction programs: Targetscan and any combination of at least four of the other prediction programs. The predicted target search examined promoter, 5′-untranslated regions, 3′-untranslated regions, and coding sequences and included a minimum seed length of 7 nucleotides (45). Using the genes selected by miRWalk, we ran a Kyoto Encyclopedia of Genes and Genomes (KEGG) pathway enrichment analysis with the use of the web-based tool DAVID (david.ncifcrf.gov/summary.jsp) (46, 47). We restricted our results to only those with ≥10 genes listed in the in silico predicted targets and an FDR q value <0.05.

RESULTS

Study Population

This study consisted of 133 women, mainly white (92%). On average, the women in our study were 30.9 ± 3.7 years of age and had a BMI of 23.6 ± 4.7 kg/m^2, and 9.4 ± 5.1 oocytes retrieved during the IVF cycle (Table 1). The majority were never smokers (54%) and 26% were current smokers. Most of the women were attempting IVF for the first time (65%).

Profile of EV-Linked miRNAs in Follicular Fluid

We screened for EV-linked miRNAs from a panel of 754 miRNAs in FF samples collected from follicles that contained mature oocytes. We detected a signal for 320 EV-linked miRNAs in at least one of the 133 FF samples analyzed. Of these, 192 EV-linked miRNAs met our predetermined threshold for inclusion and were therefore considered to be expressed. A list of the selected EV-linked miRNAs with their percentage expression levels is provided in Supplemental Table 1.

Associations Between Body Mass Index and EV-Linked miRNA Expression in Follicular Fluid

Possible associations between FF EV-linked miRNAs and BMI were investigated with the use of regression for each EV-linked miRNA. Models adjusted for age, smoking status, race, batch, and SVA surrogate variables and modeled BMI continuously. Eighteen EV-linked miRNAs were marginally significantly associated with BMI ($P<.05$; Table 2; Supplemental Table 3), and after adjusting for multiple testing, hsa-miR-328 remained significant. A 1-unit increase in BMI was associated with an increase of hsa-miR-328 expression value (ΔCt) in 0.03 standard deviation (95% confidence interval 0.02–0.05; q value 0.03).

Using Principal Component Analysis to Examine Global Variability of EV-Linked miRNA Profile

Global variability of EV-linked miRNAs was explored with the use of PCA, which revealed that the first three PCs explained >50% of the variability in the outcome data set (PC1 40%, PC2 6%, PC3 5%) (Supplemental Fig. 3). No associations were identified between smoking status, BMI, or age and these PCs in unadjusted univariate analyses; however, mutually adjusted models identified PC1 to be significantly associated with BMI ($P=.01$; Supplemental Table 4). This association remained significant after FDR (q value 0.04). To further examine the makeup of PC1, the absolute values of the PC loadings were examined (Supplemental Fig. 2; Supplemental Table 5). Twenty-five EV-linked miRNAs in PC1 with a PC loading in the 90th percentile or higher (90th percentile threshold >0.10) were identified. Six EV-linked miRNAs were identified in both the top 25 EV-linked miRNAs from PC1 and the 18 top EV-linked miRNAs from the BMI analyses (Fig. 2).

In Silico KEGG Pathways Analyses

KEGG pathways of EV-Linked miRNAs associated with BMI. We performed two KEGG analyses with the EV-linked miRNAs associated with BMI. The first examined the 18 EV-linked miRNAs that were associated with BMI in the EV-linked miRNA–by–EV-linked miRNA analysis. For this analysis, the miRWalk tool recognized 1,872 unique genes

TABLE 2

***P* value–significant EV-linked miRNAs associated with body mass index and top false-discovery rate (FDR)–significant extracellular vesicle (EV)–linked miRNA.**

EV-linked miRNA name	% expressed in population (samples)	Effect size[a]	95% CL	Unadjusted *P* value	FDR q value[b]
hsa-miR-328[c]	100% (n = 133)	0.032	(0.016, 0.048)	< .001	0.03
hsa-miR-1290	51% (n = 67)	0.049	(0.016, 0.081)	.004	0.3
hsa-miR-193b-3p	100% (n = 133)	0.03	(0.008, 0.051)	.01	0.3
hsa-miR-193b-5p	52% (n = 69)	0.035	(0.009 0.061)	.01	0.3
hsa-miR-29a	93% (n = 123)	0.018	(0.005, 0.032)	.01	0.3
hsa-miR-99b	100% (n = 133)	0.017	(0.004, 0.031)	.01	0.3
hsa-miR-331	100% (n = 133)	0.017	(0.004, 0.031)	.01	0.3
hsa-miR-423-5p	69% (n = 91)	0.028	(0.005, 0.052)	.02	0.39
hsa-miR-320a	100% (n = 133)	0.022	(0.003, 0.040)	.02	0.46
hsa-miR-720	98% (n = 130)	0.028	(0.003, 0.054)	.03	0.5
hsa-miR-28	99% (n = 131)	0.017	(0.001, 0.032)	.03	0.5
hsa-miR-483-5p	100% (n = 133)	0.027	(0.002, 0.052)	.03	0.5
hsa-miR-152	89% (n = 118)	0.018	(0.001, 0.035)	.03	0.5
hsa-miR-376a	95% (n = 126)	−0.023	(−0.045, −0.001)	.04	0.5
hsa-miR-376c	84% (n = 111)	−0.023	(−0.046, −0.001)	.04	0.5
hsa-miR-1274B	100% (n = 133)	0.026	(0.001, 0.051)	.04	0.5
hsa-miR-184	53% (n = 70)	0.023	(0.000, 0.047)	.05	0.51
hsa-miR-139-5p	71% (n = 94)	−0.024	(−0.049, 0.000)	.05	0.51

Note: Models were adjusting for age, smoking status, ethnicity, batch, and SVA surrogate variables. CL = confidence limits.
[a] For every 1-unit increase in body mass index, there is an effect size increase/decrease in standard deviation of EV-linked miRNA ΔCrt, with a lower ΔCrt indicating higher expression.
[b] FDR q value adjusted for multiple testing for the 192 EV-linked miRNAs.
[c] FDR-significant EV-linked miRNA after adjusting for multiple testing.

Martinez. BMI and EV-linked microRNAs. Fertil Steril 2019.

that were predicted from at least four prediction programs and the Targetscan software. The DAVID software identified 18 FDR-significant KEGG pathways that were associated with unique genes related to these EV-linked miRNAs. Twelve of these identified KEGG pathways are related to oocyte and follicle development and maturation (Fig. 1).

The second BMI KEGG analysis examined the 25 EV-linked miRNAs having a PC loading in the 90th percentile or above in PC1. The miRWalk software recognized 4,092 unique genes and the DAVID software found 43 KEGG pathways significantly associated with these 4,092 genes (q value <0.05). Among these 43 KEGG pathways, 24 were involved with biologic processes of interest to our study (Fig. 1).

DISCUSSION

We identified 18 EV-linked miRNAs associated with BMI. Of those, only hsa-miR-328 remained statistically significant after FDR adjustment. In addition, PCA was applied to examine the global variability in the profile of 192 EV-linked miRNAs. The first principal component explained 40% of the variability in the EV-linked miRNA dataset and was significantly associated with an increased BMI in a mutually adjusted model.

It has been well established that an increased BMI is associated with decreased fertility outcomes, such as reduced pregnancy and fertilization rates (10–12). We found hsa-miR-328 to be significantly associated with BMI after adjusting for covariates and taking into account multiple testing. Further examination of hsa-miR-328 identified associations with cancer (48, 49). MiR-328 has been known to play a role in myocardial infarction and cancers in adults, where obesity is an established risk factor (50). A study examining childhood obesity and circulating miRNAs found that circulating concentrations of hsa-miR-328 were higher in obese compared to lean children (51). This suggests that hsa-miR-328 might play a role in adipose regulation, obesity, and obesity-related diseases. A rodent study found that reducing expression of miR-328 blocked preadipocyte commitment and inducing miR-328 instigated differentiation of brown adipose tissue (52).

Few studies have examined the underlying molecular mechanisms linking BMI with fertility. One previous study assessed the associations between circulating plasma miRNAs and BMI and found 19 significant miRNAs, including hsa-miR-193b-3p (53). This was the only EV-linked miRNA overlapping with our analysis, but the directionality of the association with hsa-miR-193b-3p was the opposite of that previously reported (53). Another study examined prepregnancy BMI and circulating miRNAs during pregnancy and identified 27 significant miRNAs in two separate cohorts. Specifically, hsa-miR-28-5p, hsa-miR-376a, has-miR-139-5p, and hsa-miR-423-5p were found to overlap with those EV-linked miRNAs that were significantly associated with BMI in our analysis (54). Even more EV-linked miRNAs overlapped with Enquobahrie et al., but the direction of association was not consistent for hsa-miR-376a and hsa-miR-139-5p (54).

We also examined whether the global variability of EV-linked miRNAs was associated with BMI. EV-linked miRNAs can come from different noncoding sequences but can target the same messenger RNA transcripts (55). Thus, one EV-linked miRNA can interfere with the expression of many genes and that one gene can be negatively regulated or silenced by many EV-linked miRNAs. Our PCA identified

FIGURE 1

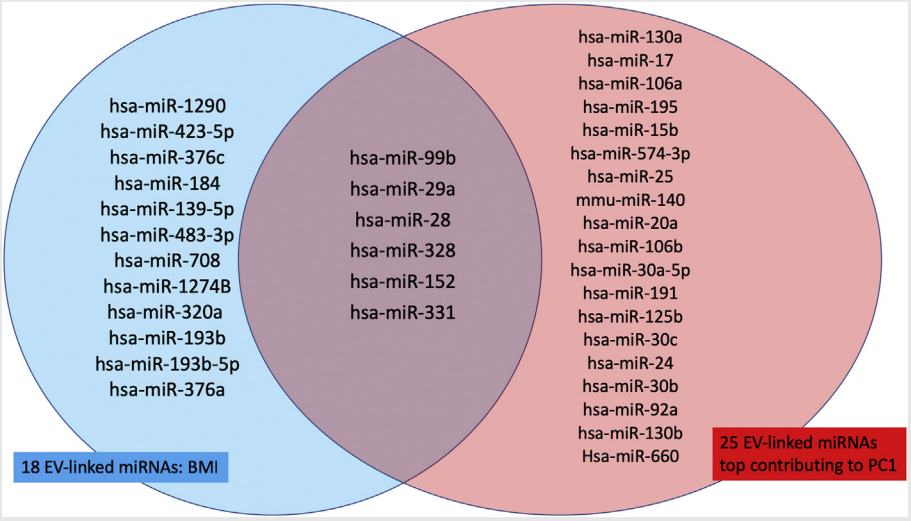

Venn diagram of EV-linked miRNAs identified in linear models and principal component (PC) analyses. Red: top identified EV-linked miRNAs associated with the 90th percentile of PC1 loadings. Blue: EV-linked miRNAs that were found to be marginally significant in linear models ($P<.05$).

Martinez. BMI and EV-linked microRNAs. Fertil Steril 2019.

PCs that would explain a certain percentage of the variability within our EV-linked miRNA dataset and found PC1 to be significantly associated with BMI. This suggests that the biologic variability captured by PC1 was significantly associated with BMI. From these two analyses, six EV-linked miRNAs overlapped as significant: hsa-miR-99b, hsa-miR-29a, hsa-miR-28, hsa-miR-328, hsa-miR-152, and hsa-miR-331. The EV-linked miRNA that was FDR significant in the EV-linked miRNA–by–EV-linked miRNA analysis, hsa-miR-328, was identified as significant in both analyses. This suggests that this hsa-miR-328 might be an important EV-linked miRNA that could be affected by an increase in BMI.

Our KEGG pathway analysis of the top EV-linked miRNAs contributing to PC1 revealed several pathways associated with pathways of cellular signaling, follicular growth, and oocyte maturation (56–60). We also performed KEGG

FIGURE 2

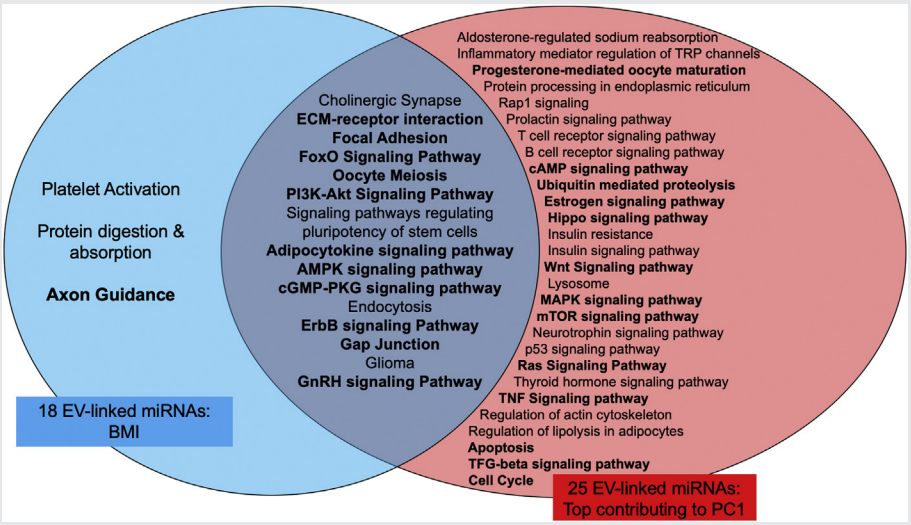

Venn diagram of false-discovery rate–significant KEGG pathways. Red: pathways identified with EV-linked miRNAs associated with the 90th percentile of PC1 loadings. Blue: pathways associated with EV-linked miRNAs and BMI. Bold indicates KEGG pathways associated with oocyte or follicle maturation, development, or fertilization.

Martinez. BMI and EV-linked microRNAs. Fertil Steril 2019.

pathway analyses on the 18 EV-linked miRNAs associated with BMI in the EV-linked miRNA–by–EV-linked miRNA regression analyses. We identified 16 significant pathways that overlapped between the three KEGG analyses. Eleven of these were associated with oocyte and follicle maturation and development: extracellular matrix (ECM)–receptor interaction, focal adhesion, FoxO signaling, oocyte meiosis, PI3K-Akt signaling, adipocytokine signaling, AMPK signaling, cGMP-PKG signaling, ErbB signaling, gap junction, and GnRH signaling pathways.

These 11 pathways contribute to oocyte development, maturation, and signaling. More notably, the Pl3K-Akt pathway has been associated with recruitment of primordial follicles, granulosa proliferation, and ovarian function (61). It also activates the mTOR and FoxO pathways (62). The FoxO pathway plays an important role in intra-oocyte signaling and can negatively regulate oocyte growth and follicular development by acting as a regulatory switch to initiate primordial follicle activation (63–66). The pathway of oocyte maturation is induced to transform an immature oocyte into a mature or fertilizable egg (67). ECM-receptor interaction is thought to play an essential role in regulating follicle development (68) and significantly contributes to follicle microenvironments that allow intracellular communication to occur between cells and the oocyte (68). Focal adhesion is necessary to establish or maintain the oocyte–granulosa cell contact in the follicle (69). Pathways identified by the significant EV-linked miRNAs play major roles in follicle and oocyte development and maturation, suggesting that BMI could disrupt these processes. This could provide a mechanistic explanation for the reduced fertility rates and increased spontaneous abortion rates that are observed with an increased BMI.

This study has limitations. First, we quantified EV-linked miRNA profiles from a single follicle, which might not accurately represent the EV-linked miRNA profile of the whole cohort of follicles. In a previous analysis (unpublished data) we compared the profile of EV-linked miRNA from two follicles per patient that contained mature oocytes and their profiles were highly correlated. Because the single follicle did not always contain the oocyte that yielded the embryo that was transferred and in many of the cases more than one embryo was transferred, we were limited in testing associations of BMI, EV-linked BMI, and pregnancy outcomes. Second, we ran our KEGG pathway analyses on a relatively small number of EV-linked miRNAs. Therefore, our results may be subject to overfitting of the selected pathways by the software. To minimize this, we set our inclusion of genes to those found in at least four separate prediction software packages in addition to the Targetscan database. We also included those EV-linked miRNAs that were marginally significant but did not meet the FDR threshold for multiple comparisons. EV-linked miRNAs are highly correlated and have high biologic variability between samples, so to prioritize biologic relevance in our pathway analyses we chose to include all those EV-linked miRNAs that met the marginally significant threshold ($P<.05$). In addition, although we can assure that we have a pellet enriched in EVs, it is possible that the pellet included not only miRNAs that are encapsulated within the EVs, but also miRNAs that were extracellularly attached to the EVs (28). In addition, there is a possibility that some of the miRNAs in the pellet derived from necrotic cells (28, 70). To ensure that we extract EV-linked miRNAs, we have optimized our protocol by running thousands of samples in previous large studies investigating EV-linked miRNAs as well as assessed random FF samples with the use of Nanosight and flow cytometry.

Our study has significant strengths as well. First, to our knowledge it is the first to examine BMI with respect to EV-linked miRNAs in FF. Second, we used PCA to examine how EV-linked miRNAs contribute to variability in our dataset, allowing us not only to expand on work done by others, but also to examine the global variability of the outcomes.

In conclusion, these identified associations between an increased BMI and FF EV-linked miRNAs may provide an insight as to how higher BMI may disrupt fertility on a mechanistic level.

REFERENCES

1. Mascarenhas MN, Flaxman SR, Boerma T, Vanderpoel S, Stevens GA. National, regional, and global trends in infertility prevalence since 1990: a systematic analysis of 277 health surveys. PLoS Med 2012;9:e1001356.
2. Rossi BV, Abusief M, Missmer SA. Modifiable risk factors and infertility: what are the connections? Am J Lifestyle Med 2014;10:220–31.
3. Klonoff-Cohen H. Female and male lifestyle habits and IVF: what is known and unknown. Hum Reprod Update 2005;11:179–203.
4. Hornstein MD. Lifestyle and IVF outcomes. Reprod Sci 2016;23:1626–9.
5. Frattarelli JL, Kodama CL. Impact of body mass index on in vitro fertilization outcomes. J Assist Reprod Genet 2004;21:211–5.
6. Jungheim ES, Macones GA, Odem RR, Patterson BW, Lanzendorf SE, Ratts VS, et al. Associations between free fatty acids, cumulus oocyte complex morphology and ovarian function during in vitro fertilization. Fertil Steril 2011;95:1970–4.
7. Matalliotakis I, Cakmak H, Sakkas D, Mahutte N, Koumantakis G, Arici A. Impact of body mass index on IVF and ICSI outcome: a retrospective study. Reprod Biomed Online 2008;16:778–83.
8. Robker RL. Evidence that obesity alters the quality of oocytes and embryos. Pathophysiology 2008;15:115–21.
9. Esinler I, Bozdag G, Yarali H. Impact of isolated obesity on ICSI outcome. Reprod Biomed Online 2008;17:583–7.
10. Petanovski Z, Dimitrov G, Ajdin B, Hadzi-Lega M, Sotirovska V, Matevski V, et al. Impact of body mass index (BMI) and age on the outcome of the IVF process. Prilozi 2011;32:155–71.
11. Lintsen AM, Pasker-de Jong PC, de Boer EJ, Burger CW, Jansen CA, Braat DD, et al. Effects of subfertility cause, smoking and body weight on the success rate of IVF. Hum Reprod 2005;20:1867–75.
12. Bellver J, Ayllon Y, Ferrando M, Melo M, Goyri E, Pellicer A, et al. Female obesity impairs in vitro fertilization outcome without affecting embryo quality. Fertil Steril 2010;93:447–54.
13. Rimon-Dahari N, Yerushalmi-Heinemann L, Alyagor L, Dekel N. Ovarian folliculogenesis. In: Piprek RP, editor. Molecular mechanisms of cell differentiation in gonad development. Cham: Springer International Switzerland; 2016:167–90.
14. Hennet ML, Combelles CM. The antral follicle: a microenvironment for oocyte differentiation. Int J Dev Biol 2012;56:819–31.
15. Machtinger R, Laurent LC, Baccarelli AA. Extracellular vesicles: roles in gamete maturation, fertilization and embryo implantation. Hum Reprod Update 2016;22:182–93.
16. Fortune JE. Ovarian follicular growth and development in mammals. Biol Reprod 1994;50:225–32.

17. Scalici E, Traver S, Molinari N, Mullet T, Monforte M, Vintejoux E, et al. Cell-free DNA in human follicular fluid as a biomarker of embryo quality. Hum Reprod 2014;29:2661–9.
18. Baka S, Malamitsi-Puchner A. Novel follicular fluid factors influencing oocyte developmental potential in IVF: a review. Reprod Biomed Online 2006;12: 500–6.
19. De Placido G, Alviggi C, Clarizia R, Mollo A, Alviggi E, Strina I, et al. Intrafollicular leptin concentration as a predictive factor for in vitro oocyte fertilization in assisted reproductive techniques. J Endocrinol Invest 2006;29: 719–26.
20. Revelli A, Piane LD, Casano S, Molinari E, Massobrio M, Rinaudo P. Follicular fluid content and oocyte quality: from single biochemical markers to metabolomics. Reprod Biol Endocrinol 2009;7:40.
21. Machtinger R, Rodosthenous RS, Adir M, Mansour A, Racowsky C, Baccarelli AA, et al. Extracellular microRNAs in follicular fluid and their potential association with oocyte fertilization and embryo quality: an exploratory study. J Assist Reprod Genet 2017;34:525–33.
22. Weber JA, Baxter DH, Zhang S, Huang DY, How Huang K, Jen Lee M, et al. The microRNA spectrum in 12 body fluids. Clin Chem 2010;56:1733–41.
23. Tannetta D, Dragovic R, Alyahyaei Z, Southcombe J. Extracellular vesicles and reproduction—promotion of successful pregnancy. Cell Mol Immunol 2014;11:548–63.
24. Lim LP, Lau NC, Garrett-Engele P, Grimson A, Schelter JM, Castle J, et al. Microarray analysis shows that some microRNAs downregulate large numbers of target mRNAs. Nature 2005;433:769.
25. Li SC, Tang P, Lin WC. Intronic microRNA: discovery and biological implications. DNA Cell Biol 2007;26:195–207.
26. Sætrom P, Snøve O Jr, Rossi JJ. Epigenetics and microRNAs. Pediatr Res 2007;61:17R.
27. Raposo G, Stoorvogel W. Extracellular vesicles: exosomes, microvesicles, and friends. J Cell Biol 2013;200:373–83.
28. Hill AF, Pegtel DM, Lambertz U, Leonardi T, O'Driscoll L, Pluchino S, et al. ISEV position paper: extracellular vesicle RNA analysis and bioinformatics. J Extracell Vesicles 2013;2 https://doi.org/10.3402/jev.v2i0.22859.
29. Di Pietro C. Exosome-mediated communication in the ovarian follicle. J Assist Reprod Genet 2016;33:303–11.
30. Yáñez-Mó M, Siljander PRM, Andreu Z, Bedina Zavec A, Borràs FE, Buzas EI, et al. Biological properties of extracellular vesicles and their physiological functions. J Extracell Vesicles 2015;4:27066.
31. Ferrante SC, Nadler EP, Pillai DK, Hubal MJ, Wang Z, Wang JM, et al. Adipocyte-derived exosomal miRNAs: a novel mechanism for obesity-related disease. Pediatr Res 2015;77:447–54.
32. Bollati V, Iodice S, Favero C, Angelici L, Albetti B, Cacace R, et al. Susceptibility to particle health effects, miRNA and exosomes: rationale and study protocol of the SPHERE study. BMC Public Health 2014;14:1137.
33. Shi X-F, Wang H, Kong F-X, Xu Q-Q, Xiao F-J, Yang Y-F, et al. Exosomal miR-486 regulates hypoxia-induced erythroid differentiation of erythroleukemia cells through targeting Sirt1. Exp Cell Res 2017;351:74–81.
34. Jones A, Danielson KM, Benton MC, Ziegler O, Shah R, Stubbs RS, et al. miRNA signatures of insulin resistance in obesity. Obesity (Silver Spring) 2017;25:1734–44.
35. World Medical Association. Declaration of Helsinki: ethical principles for medical research involving human subjects. JAMA 2013;310:2191–4.
36. Ferraretti AP, La Marca A, Fauser BC, Tarlatzis B, Nargund G, Gianaroli L, et al. ESHRE consensus on the definition of 'poor response' to ovarian stimulation for in vitro fertilization: the Bologna criteria. Hum Reprod 2011;26: 1616–24.
37. Witwer KW, Buzas EI, Bemis LT, Bora A, Lasser C, Lotvall J, et al. Standardization of sample collection, isolation and analysis methods in extracellular vesicle research. J Extracell Vesicles 2013;2.
38. Pergoli L, Cantone L, Favero C, Angelici L, Iodice S, Pinatel E, et al. Extracellular vesicle–packaged miRNA release after short-term exposure to particulate matter is associated with increased coagulation. Part Fibre Toxicol 2017; 14:32.
39. Gardiner C, di Vizio D, Sahoo S, Thery C, Witwer KW, Wauben M, et al. Techniques used for the isolation and characterization of extracellular vesicles: results of a worldwide survey. J Extracell Vesicles 2016;5:32945.
40. Enderle D, Spiel A, Coticchia CM, Berghoff E, Mueller R, Schlumpberger M, et al. Characterization of RNA from exosomes and other extracellular vesicles isolated by a novel spin column-based method. PLoS One 2015;10: e0136133.
41. Leek JT, Johnson WE, Parker HS, Jaffe AE, Storey JD. The SVA package for removing batch effects and other unwanted variation in high-throughput experiments. Bioinformatics 2012;28:882–3.
42. Jeffery T, Leek WEJ, Parker HS, Fertig EJ, Jaffe AE, Storey JD, et al. SVA: surrogate variable analysis, In: Vol. package version 3.24.4. Vienna: R Foundation for Statistical Computing; 2017.
43. Benjamini Y, Hochberg Y. Controlling the false discovery rate: a practical and powerful approach to multiple testing. J R Stat Soc Ser B Stat [Methodol] 1995;57:289–300.
44. R Core Team. R: a language and environment for statistical computing. Vienna: R Foundation for Statistical Computing; 2017.
45. Dweep H, Sticht C, Pandey P, Gretz N. miRWalk—database: prediction of possible miRNA binding sites by "walking" the genes of three genomes. J Biomed Inform 2011;44:839–47.
46. Huang DW, Sherman BT, Lempicki RA. Systematic and integrative analysis of large gene lists using DAVID bioinformatics resources. Nat Protoc 2008; 4:44.
47. Huang DW, Sherman BT, Lempicki RA. Bioinformatics enrichment tools: paths toward the comprehensive functional analysis of large gene lists. Nucleic Acids Res 2009;37:1–13.
48. Wu Z, Sun L, Wang H, Yao J, Jiang C, Xu W, et al. MiR-328 Expression is decreased in high-grade gliomas and is associated with worse survival in primary glioblastoma. PLoS One 2012;7:e47270.
49. Ishimoto T, Sugihara H, Watanabe M, Sawayama H, Iwatsuki M, Baba Y, et al. Macrophage-derived reactive oxygen species suppress miR-328 targeting CD44 in cancer cells and promote redox adaptation. Carcinogenesis 2014;35:1003–11.
50. Brettfeld C, Maver A, Aumuller E, Peterlin B, Haslberger AG. MicroRNAs responsible for inflammation in obesity. J Endocrinol Metab 2017;7: 77–85.
51. Prats-Puig A, Ortega FJ, Mercader JM, Moreno-Navarrete JM, Moreno M, Bonet N, et al. Changes in circulating microRNAs are associated with childhood obesity. J Clin Endocrinol Metab 2013;98:E1655–60.
52. Oliverio M, Schmidt E, Mauer J, Baitzel C, Hansmeier N, Khani S, et al. Dicer1-miR-328-Bace1 signalling controls brown adipose tissue differentiation and function. Nat Cell Biol 2016;18:328–36.
53. Ameling S, Kacprowski T, Chilukoti RK, Malsch C, Liebscher V, Suhre K, et al. Associations of circulating plasma microRNAs with age, body mass index and sex in a population-based study. BMC Med Genom 2015;8:61.
54. Enquobahrie DA, Wander PL, Tadesse MG, Qiu C, Holzman C, Williams MA. Maternal pre-pregnancy body mass index and circulating microRNAs in pregnancy. Obes Res Clin Pract 2017;11:464–74.
55. Bartel DP. MicroRNA Target Recognition and regulatory functions. Cell 2009;136:215–33.
56. Knight PG, Glister C. Local roles of TGF-beta superfamily members in the control of ovarian follicle development. Anim Reprod Sci 2003;78:165–83.
57. Boyer A, Goff AK, Boerboom D. WNT signaling in ovarian follicle biology and tumorigenesis. Trends Endocrinol Metab 2010;21:25–32.
58. Boerboom D, Paquet M, Hsieh M, Liu J, Jamin SP, Behringer RR, et al. Misregulated Wnt/beta-catenin signaling leads to ovarian granulosa cell tumor development. Cancer Res 2005;65:9206–15.
59. Zhang M, Ouyang H, Xia G. The signal pathway of gonadotrophins-induced mammalian oocyte meiotic resumption. Mol Hum Reprod 2009; 15:399–409.
60. Conti M, Hsieh M, Zamah AM, Oh JS. Novel signaling mechanisms in the ovary during oocyte maturation and ovulation. Mol Cell Endocrinol 2012; 356:65–73.
61. Andrade GM, da Silveira JC, Perrini C, Del Collado M, Gebremedhn S, Tesfaye D, et al. The role of the PI3K-Akt signaling pathway in the developmental competence of bovine oocytes. PLoS One 2017;12:e0185045.
62. Makker A, Goel MM, Mahdi AA. PI3K/PTEN/Akt and TSC/mTOR signaling pathways, ovarian dysfunction, and infertility: an update. J Mol Endocrinol 2014;53:R103–18.

63. Liu L, Rajareddy S, Reddy P, Du C, Jagarlamudi K, Shen Y, et al. Infertility caused by retardation of follicular development in mice with oocyte-specific expression of Foxo3a. Development 2007;134:199–209.
64. Pelosi E, Omari S, Michel M, Ding J, Amano T, Forabosco A, et al. Constitutively active Foxo3 in oocytes preserves ovarian reserve in mice. Nat Commun 2013;4:1843.
65. Brenkman AB, Burgering BM. Foxo3a eggs on fertility and aging. Trends Mol Med 2003;9:464–7.
66. John GB, Gallardo TD, Shirley LJ, Castrillon DH. Foxo3 is a PI3K-dependent molecular switch controlling the initiation of oocyte growth. Dev Biol 2008;321:197–204.
67. Schmitt A, Nebreda AR. Signalling pathways in oocyte meiotic maturation. J Cell Sci 2002;115:2457.
68. Woodruff TK, Shea LD. The role of the extracellular matrix in ovarian follicle development. Reprod Sci (Thousand Oaks) 2007;14:6–10.
69. McGinnis LK, Kinsey WH. Role of focal adhesion kinase in oocyte-follicle communication. Mol Reprod Dev 2015;82:90–102.
70. Endzelins E, Berger A, Melne V, Bajo-Santos C, Sobolevska K, Abols A, et al. Detection of circulating miRNAs: comparative analysis of extracellular vesicle-incorporated miRNAs and cell-free miRNAs in whole plasma of prostate cancer patients. BMC Cancer 2017;17:730.

Relación entre el índice de masa corporal y los microRNAs ligados a vesículas extracelulares del líquido folicular humano

Objetivo: Estudiar si un aumento en el índice de masa corporal (IMC) está asociado con una expresión alterada de los microRNAs asociados a vesículas extracelulares (EVlinked miRNAs) en el líquido folicular humano.

Diseño: Estudio transversal.

Ámbito: Centro universitario de atención terciaria.

Paciente(s): Se reclutaron 133 mujeres sometidas a un ciclo de fecundación in vitro (FIV) entre enero de 2014 y agosto de 2016.

Intervención(es): Ninguna.

Principal(es) medida(s) de resultado(s): Se aislaron los EV-linked miRNAs del líquido folicular y se midió su perfil de expresión mediante el uso de un panel Taqman Open Array Human miRNA. Los EV-linked miRNAs fueron globalmente normalizados y transformados de forma inversamente-normal. La relación entre el índice de masa corporal (IMC) y el resultado de los EV-linked miRNA se analizó mediante regresión lineal multivariante y análisis de componentes principales.

Resultados (s): Tras hacer un ajuste por edad, etnia, hábito de fumar y lotes, se observó una relación entre 18 EV-linked miRNAs y un aumento del IMC. Los Hsa-miR-328 permanecieron significativos tras los ajustes de hallazgos falsos. El análisis de componentes principales identificó el principal componente responsable de una variación del 40% en nuestro conjunto de datos de EV-linked miRNA, y ajustando mediante regresión lineal se encontró que el componente principal estaba asociado con el IMC, tras ajustes de pruebas múltiples. Utilizando la enciclopedia Kyoto de genes y análisis enriquecido del genoma, predijimos genes dianas de EV-linked miRN *in silico* e identificamos la señalización de PI3K-Akt, la interacción con el receptor matriz extracelular (ECM), la adhesión focal, la señalización Fox0 y los circuitos de la meiosis ovocitaria.

Conclusión (es): Estos resultados demuestran que el aumento de 1 unidad en el IMC está asociado con la expresión alterada de EV-linked miRNAs en el líquido, el cual puede influir en vías implicadas en el desarrollo folicular y ovocitario. Nuestros hallazgos proporcionan una percepción potencial sobre una explicación mecánica de la reducción de la fertilidad asociada a un elevado IMC.

SUPPLEMENTAL FIGURE 1

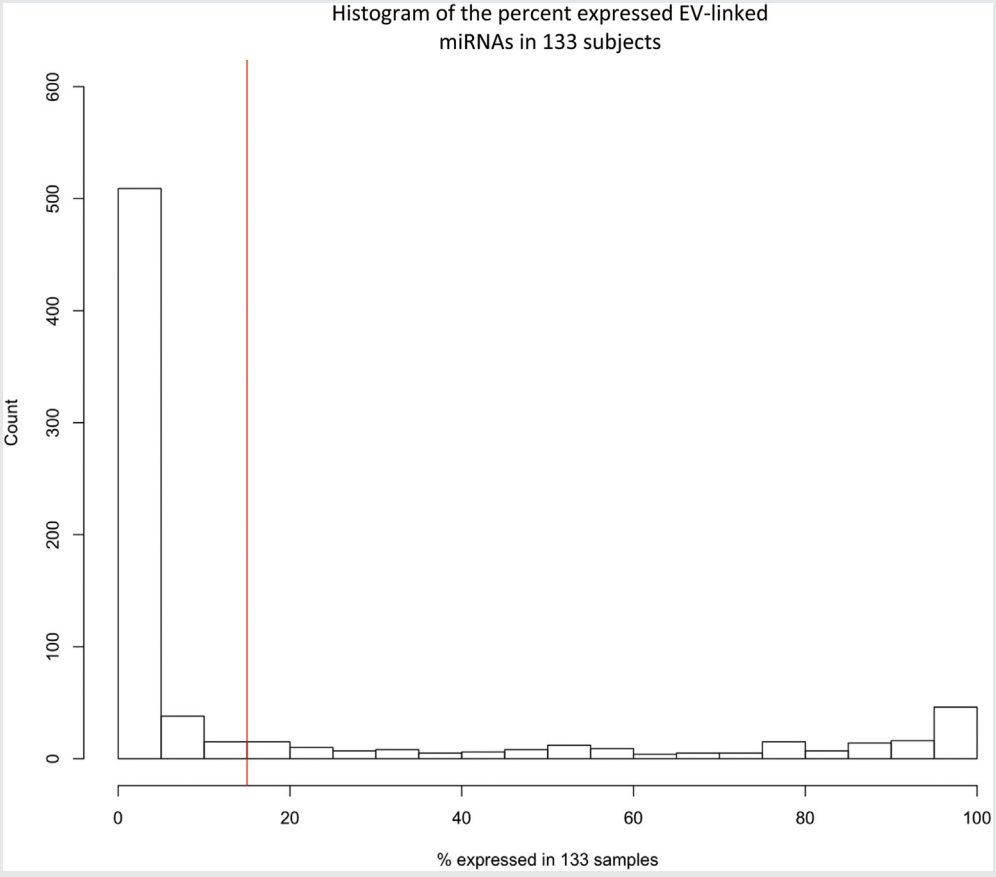

Histogram of percentage detected levels of expression of each EV-linked miRNA. Red line denotes the 15% threshold which separates the majority of expressed EV-linked miRNAs (to the right of the line) from those that did not express (to the left of the line).

Martinez. BMI and EV-linked microRNAs. Fertil Steril 2019.

SUPPLEMENTAL FIGURE 2

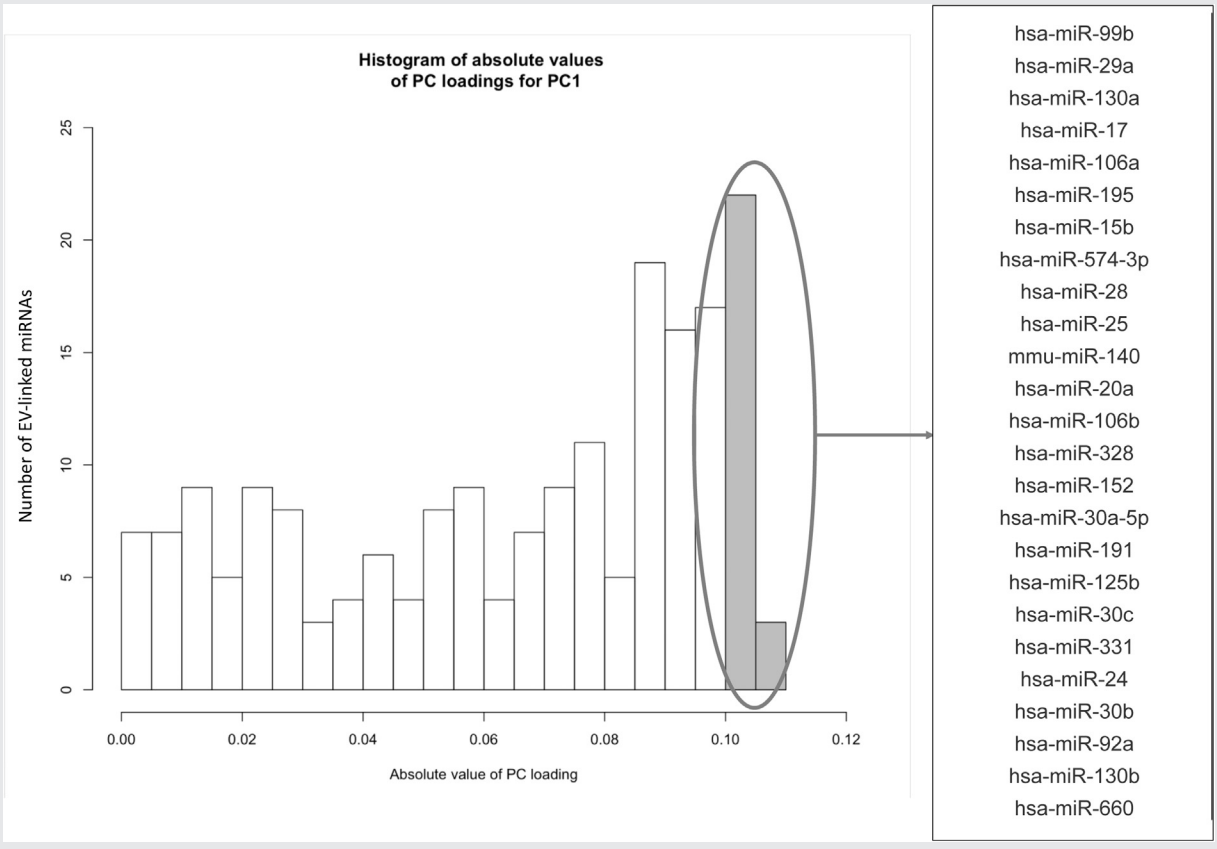

Histogram of the absolute values of the principal component (PC) loadings from PC1. Bars indicate the 90th percentile or higher of PC loadings. EV-linked miRNAs examined in this percentile are listed.

Martinez. BMI and EV-linked microRNAs. Fertil Steril 2019.

SUPPLEMENTAL FIGURE 3

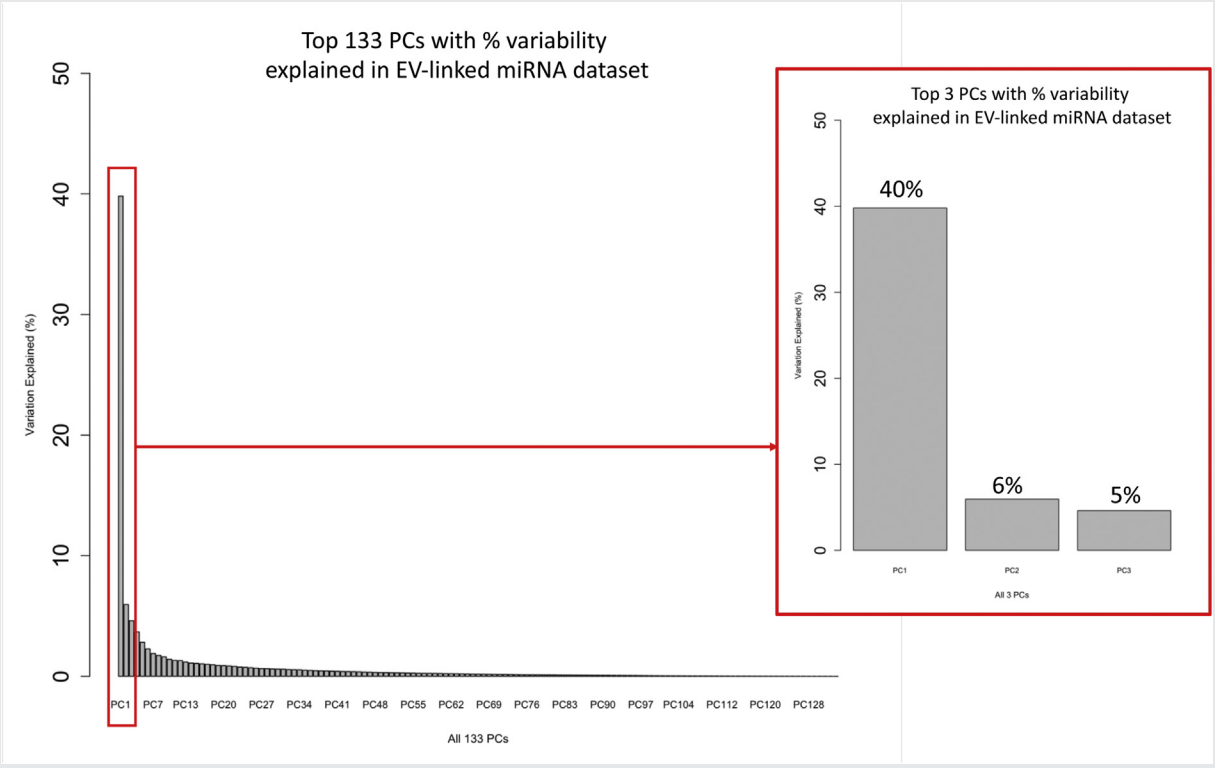

Principal components (PCs) from PC analysis. On the left, all 133 principal components calculated with the *y*-axis showing the percentage of variability that each PC explains in the EV-linked miRNA dataset. On the right, a close-up of the top three PCs with their percentage of variability described.

Martinez. BMI and EV-linked microRNAs. Fertil Steril 2019.